AN EXTRAPOLATION METHOD FOR REDUCING EQUILIBRATION TIMES IN SEDIMENTATION EQUILIBRIUM EXPERIMENTS

JOHN J. CORREIA AND DAVID A. YPHANTIS, *Biochemistry and Biophysics Section, Biological Sciences Group and Institute of Materials Science, University of Connecticut, Storrs, Connecticut 06268,* AND
GEORGE H. WEISS, *Physical Sciences Laboratory, Division of Computer Research and Technology, National Institutes of Health, Bethesda, Maryland 20014 U. S. A.*

ABSTRACT We present a detailed investigation of the use of an extrapolation technique to decrease running times of sedimentation equilibrium experiments. If concentration profiles are available at time $\Delta\tau, 2\Delta\tau, 3\Delta\tau, \ldots, c_n(r) = c(r, n\Delta\tau)$, then the Aitken transformation replaces the $c_n(r)$ by $\hat{c}_n(r) = [c_{n+1}(r)c_{n-1}(r) - c_n^2(r)]/[c_{n+1}(r) + c_{n-1}(r) - 2c_n(r)]$. We show that the $\hat{c}_n(r)$ converge to the equilibrium values $c_\infty(r)$ much more quickly than the $c_n(r)$. Savings in time are shown to range from a factor of approximately 2 for meniscus depletion experiments to factors of between 4 and 8 for lower speeds or smaller molecular weights. It is also shown that the technique is quite sensitive to noise, so that an accurate optical system is required to allow its optimal use.

INTRODUCTION

A potential drawback in the use of equilibrium sedimentation experiments, especially for unstable systems, is the length of time required to attain equilibrium. The short-column approach proposed by van Holde and Baldwin (1) and further implemented by one of us (2) can greatly decrease the time required at the expense of somewhat reduced accuracy and loss of potentially useful higher molecular moments. Overspeeding procedures (3, 4) can speed up the attainment of equilibrium spectacularly, but they require prior knowledge of the parameters of the system and careful control of experimental procedures (4). These overspeeding procedures may prove useless or can even extend the equilibrium times if some components of the system are "pelleted" at the speeds used and precipitate out of solution or form gels at the base of a cell. Griffith (5) recommends the experimental approximation of the final concentration distribution by the simultaneous formation of a number of synthetic boundaries in the ultracentrifuge cell. This procedure appears to be quite effective but also requires prior knowledge of the system to be measured in order to take full advantage of the procedure.

Baurain et al. (6) have proposed experimental estimation of the equilibrium concentration differences across the solution column by the extrapolation to infinite time of the differences observed during the approach to equilibrium. They assumed that the

concentration distributions (at sufficiently large times) can be described as the sum of the equilibrium distribution and of the first eigenfunctions. This assumption appears to be generally valid, as Archibald (7) showed for single-component ideal systems and as has been predicted for a number of nonideal systems (8, 9) and self-associating systems[1] at sufficiently large times. The procedure of Baurain et al. uses a successive approximation technique to estimate the equilibrium concentration difference across the solution column. As described, this procedure yields only the weight-average molecular weight. We present here a more general approach for predicting the equilibrium distributions throughout the whole solution column and illustrate this procedure with data obtained by numerical solutions of the Lamm equation for various types of systems. Experimental implementation of this suggestion could provide a means for ultracentrifugal characterization of unstable preparations because of the shorter equilibration times involved.

THEORY

The concentration profile for many systems can be expressed as

$$c(r,t) = c(r,\infty) + \sum_{j=1}^{\infty} A_j(r)\exp(-\lambda_j t). \tag{1}$$

where t is the time, r is radial position, and the λ_j are real, positive, eigenvalues that can be ordered as $\lambda_1 < \lambda_2 < \lambda_3 < \ldots$. To motivate the following analysis, notice that if one could eliminate the first eigenvalue term, the approach to equilibrium would be more rapid because the second term decays to zero more quickly. A nonlinear transformation due to Aitken (10) accomplishes just that elimination. Suppose that r is fixed and measurements of $c(r,t)$ are available at times $t_n = n\Delta t$, $n = 1,2,3,\ldots$. Let the corresponding values of $c(r,t)$ be denoted by c_n. Then if we consider the sequence

$$\hat{c}_n = \frac{c_{n+1}c_{n-1} - c_n^2}{c_{n+1} + c_{n-1} - 2c_n}, \tag{2}$$

it will be found that the sequence $\hat{c}_n$ converges to $c(r,\infty)$ more rapidly than the original sequence of values. A similar transformation can be made for the concentration gradient. This transformation can be considered equivalent to fitting the concentrations observed for each radius at three equispaced times to a single exponential relaxation, independently of the behavior at any other radius, and thus it is subject to the same restraints and pitfalls as a three-point fitting procedure.

Two remarks are in order at this point. First, the efficiency of the method depends on how well separated the λ's are. Analysis of results from the rectangular approximation (8) and of our previous equilibrium system studies (9)[1] shows that the eigenvalues are well separated for most sedimentation equilibrium experiments involving a single sedimenting chemical component. Secondly, there is a loss of accuracy asso-

[1]Johnson, M. L., G. H. Weiss, and D. A. Yphantis. 1976. Unpublished results.

ciated with the use of Eq. 2 because of the second difference of the c_n appearing in the denominator. Hence one needs to start with intrinsically accurate data. If the data were completely noise-free, then one could use higher-order analogues of Eq. 2 to reduce the time to equilibrium even more dramatically (12). The noise is, however, the limiting factor. Notice that although we started by assuming that $c(r, t)$ can be written as an eigenfunction expansion, this need never be ascertained directly since the algorithm of Eq. 2 is a strictly numerical one. Hence one need only calculate the successive $\hat{c}_n$ to see whether they approach a constant value that should be the equilibrium concentration.

If we rewrite Eq. 1 as

$$c_n = c_\infty + A\beta^n + R_n, \tag{3}$$

where $\beta = \exp(-\lambda\Delta t)$, then c_n is found to be

$$\hat{c}_n = c_\infty + \frac{\left(\beta R_{n-1} + \frac{1}{\beta} R_{n+1} - 2R_n\right) + (R_{n+1}R_{n-1} - R_n^2)/(A\beta^n)}{(\beta + 1/\beta - 2) + (R_{n+1} + R_{n-1} - 2R_n)/(A\beta^n)}, \tag{4}$$

so that, when the R_n are smaller than $A\beta^n$, $c_n - c$ is roughly of the order of R_n rather than being of the order of $A\beta^n$, which would be the case if the original concentrations were used for the extrapolation. It should be noted that the R_n in Eq. 4 can also represent arbitrary deviations, such as random error, so that the evaluation of Eq. 2 is not seriously degraded as all concentrations approach the equilibrium value, even though it may appear that Eq. 2 essentially requires a division by (a noise-modulated) zero (*vide infra*). The error in the estimated concentration is least when r is such that $A(r)$ vanishes. In the rectangular approximation the value of R_n, at sufficiently large time, can roughly be represented as $R_n = B\beta^{4n}$, in which case Eq. 4 becomes

$$\hat{c}_n \sim c_\infty + \frac{AB\beta^{4n-2}(1 - \beta^3)^2}{A(1 - \beta)^2 + B\beta^{3n-3}(1 - \beta^4)^2}, \tag{5}$$

as compared to $c_n \sim c_\infty + A\beta^n$.

To give a quantitative estimate of the degree of improvement in a somewhat less abstract way, we compare results of the present transformation with those calculated by van Holde and Baldwin for the rate of approach to equilibrium of an ideal, nondisperse system. As a measure of closeness to equilibrium, they define a parameter ϵ in terms of the difference in concentration between meniscus and base, Δc_r:

$$\epsilon = 1 - \Delta c_r/\Delta c_\infty. \tag{6}$$

They showed that the time to reach the value could be expressed as

$$t_\epsilon = [(r_2 - r_1)^2/D]\,F(\alpha), \tag{7}$$

where r_1 and r_2 are the positions of the meniscus and base, respectively, D is the diffusion constant, and $F(\alpha)$ is a dimensionless function of the parameter $\alpha = 2D/[s\omega^2 \cdot$

$(r_2^2 - r_1^2)]$ and of ϵ. Introducing the dimensionless reduced effective centrifugation time, $\tau = 2\omega^2 s_0 t$ (where ω is the angular velocity and s_0 the sedimentation coefficient at infinite dilution), we can write the van Holde-Baldwin formula as

$$\tau_\epsilon = -[1/\pi^2\alpha\gamma U(\alpha)] \ln [\pi^2 U^2(\alpha)\epsilon/4(1 + \cosh(1/2\alpha))] \quad (8)$$

where

$$U(\alpha) = 1 + 1/4\pi^2\alpha^2 \text{ and } \gamma = \tfrac{1}{4}[(r_2 + r_1)/(r_2 - r_1)] \quad (9)$$

Suppose now, that we make an Aitken transformation every $\Delta\tau$ units of the dimenless time, then the comparable convergence of the predicted equilibrium concentration $\hat{c}(\tau)$, i.e., $\epsilon' = 1 - \Delta\hat{c}_\tau/\Delta c$, will be attained when

$$\tau'_\epsilon = -\frac{1}{4\pi^2\alpha\gamma V(\alpha)} \ln \left[\frac{\pi^2 V^2(\alpha)\epsilon}{\cosh\left(\frac{1}{2\alpha}\right) - 1} \left(\frac{\cosh(\pi^2\alpha\gamma V(\alpha)\Delta\tau) - 1}{\cosh(3\pi^2\alpha\gamma\Delta\tau) - 1} \right) \right]. \quad (10)$$

Here $V(\alpha) = 1 + 1/(16\pi^2\alpha^2)$. Fig. 1 presents the ratios of $\tau'_\epsilon/\tau_\epsilon$, the equilibrium times given by Eqs. 10 and 8, for $\Delta\tau = 10^{-4}$ and for $\epsilon = 10^{-2}$, 10^{-3}, and 10^{-4} as a function of α. For the usual sedimentation equilibrium experiment $\alpha \sim 1$, and under these conditions there is an approximate sixfold saving in time through the use of Aitken transformation. On the other hand, "high-speed" equilibrium (meniscus de-

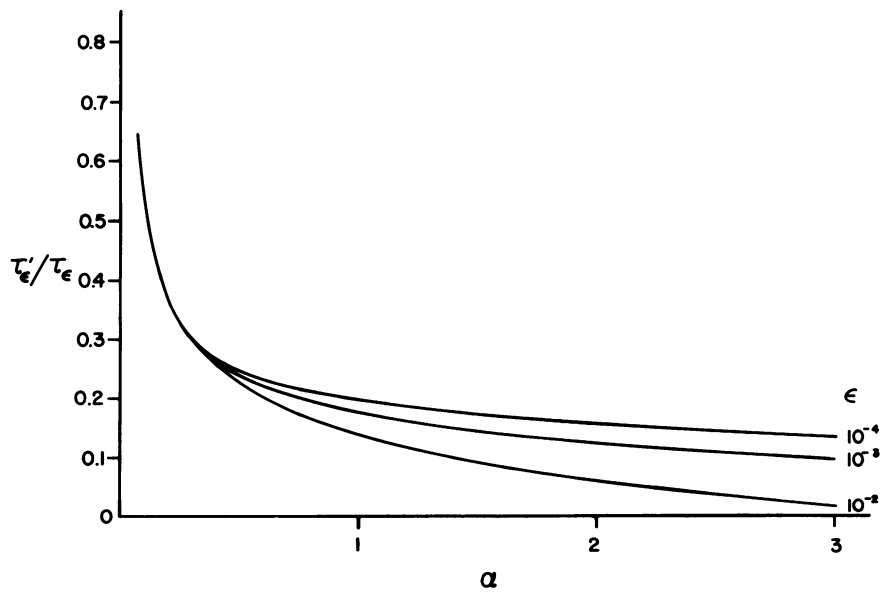

FIGURE 1 Ratio of the extrapolated time to equilibrium in the concentration difference across the cell to the time required to attain equilibrium for the same ϵ, plotted as a function of $\alpha = 2RT/[M(1 - \bar{v}\rho)(r_2^2 - r_1^2)]$. For the usual sedimentation equilibrium experiments $\alpha \sim 1$; for meniscus depletion experiments $\alpha \approx 0.1$. These curves, for $\Delta\tau = 10^{-4}$, are typical of observations very close in time.

pletion) experiments correspond to $\alpha \sim 0.1$ and under these conditions there is less than a twofold decrease in the time required to estimate the equilibrium concentrations.

NUMERICAL ILLUSTRATIONS

The results to be presented all pertain to the Lamm equation:

$$\frac{\partial c}{\partial \tau} = \frac{1}{2r}\frac{\partial}{\partial r}\left[\frac{r}{\sigma_0}\frac{\partial c}{\partial r} - r^2 f(c)c\right], \tag{11}$$

where $\sigma_0 = \omega^2 s_0 / D$ and $s = s_0 f(c)$ is the sedimentation coefficient at concentration c. Numerical solutions of Eq. 11 were generated by a finite difference scheme described earlier (9, 13). In all cases the meniscus, r_1, and the base, r_2, of the solution column were fixed at 6.4 and 6.7 cm, respectively, values typical of most ordinary (1) and high-speed (14) sedimentation equilibrium experiments. In Fig. 2 we present results for $\sigma = \omega^2 s_0 / D = 0.509\ \text{cm}^{-2}$ for the ideal case $s = s_0$ (i.e., $f(c) = 1$). Fig. 2 *a* follows the time-course of $c(r, \tau)$ and $\hat{c}(r, \tau)$ for a value of r near the meniscus and for $\Delta\tau = 10^{-3}$ for noise-free data. It is clear that by $\tau = 0.02$, $\hat{c}(r, \tau)$ has converged to its equilibrium value, while $c(r, \tau)$ reaches the same value at $\tau \sim 0.07$. Fig. 2 *b* presents comparable curves for a point near the base. It is interesting to note that $c(r, \tau)$ here overshoots c_∞ before approaching it, although the savings in time are again quite dramatic. Curves of $| c(r, \tau) - c(r, \infty) |$ and $| \hat{c}(r, \tau) - \hat{c}(r, \infty) |$ are presented as a function of τ for these two points in Figs. 2 *c* and 2 *d* respectively. The approach to equilibrium is seen to be exponential, and the difference in time constants for $c(r, \tau)$ and its transform $\hat{c}(r, \tau)$ is obvious. The discontinuity in Fig. 2 *d* corresponds to the overshoot seen, in linear scale, in Fig. 2 *b*.

In Fig. 3 *a* and 3 *b* we examine the effect of varying $\Delta\tau$ on the approach to equilibrium, of the same system whose behavior is described in Figs. 2 *a* and 2 *b*. The requirement of minimizing the effect of noise prescribes as large a value of $\Delta\tau$ as possible (*vide infra*) while the optimal speed of approach to equilibrium requires that $\Delta\tau$ be as small as possible. The results in Fig. 3 indicate that variations in $\Delta\tau$ do not greatly affect the extrapolation to equilibrium, so that sensitivity to noise should be the principal determinant of the value of $\Delta\tau$.

NONLINEAR SYSTEMS

Numerical solutions to the Lamm equation were generated for several other conditions and Eq. 2 was used to provide estimates of the equilibrium distributions as a function of time. In all cases there were significant savings in equilibration time by all criteria examined. For example the application of the Aitken transformation to simple nonideal systems, where $s(c)/s_0 = f(c) = 1/(1 + kc)$ reduced the equilibration times by factors ranging from 4 to 8 for $\alpha \sim 1$. The van Holde-Baldwin criterion and its analogue were used for all these comparisons and the savings in time depended on the exact conditions assumed, as shown in Table I.

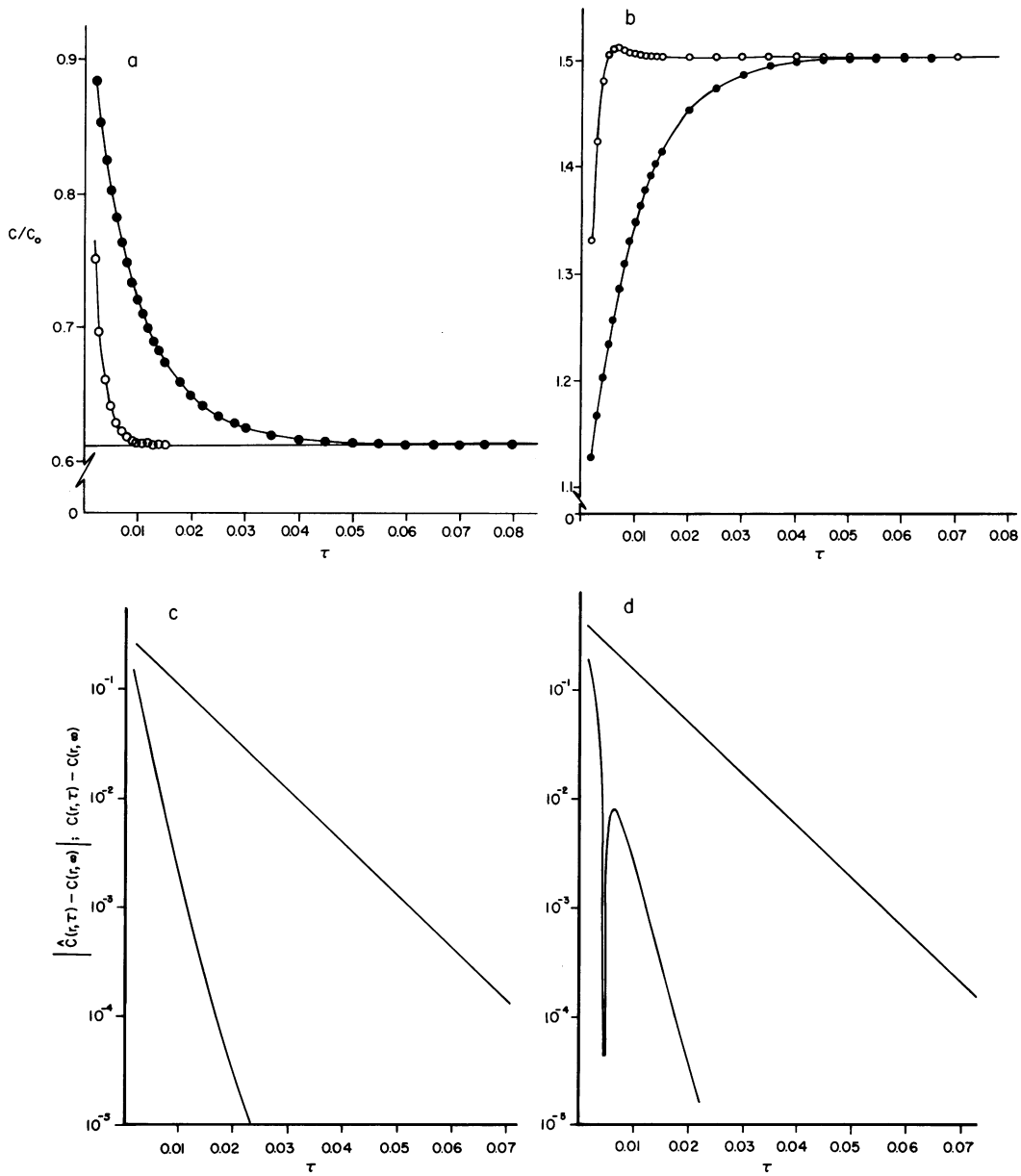

FIGURE 2 Approach to equilibrium for observed concentrations and estimated concentrations. Data calculated for an ideal system with $\sigma_0 = \omega^2 s_0 / D = 0.509\ \text{cm}^{-2}$ ($\alpha = 1$) and $\Delta\tau = 10^{-3}$ (a, c) at 6.415 cm, near the meniscus, and (b, d) at 6.585 cm, near the base of the solution column. The concentrations are presented on a linear scale in panels a and b and in panels c and d as the logarithm of the absolute value of the difference between the equilibrium and transient values. Note that the overshoot in $\hat{c}(6.685, \tau)$ of panel b is reflected in the discontinuity of d.

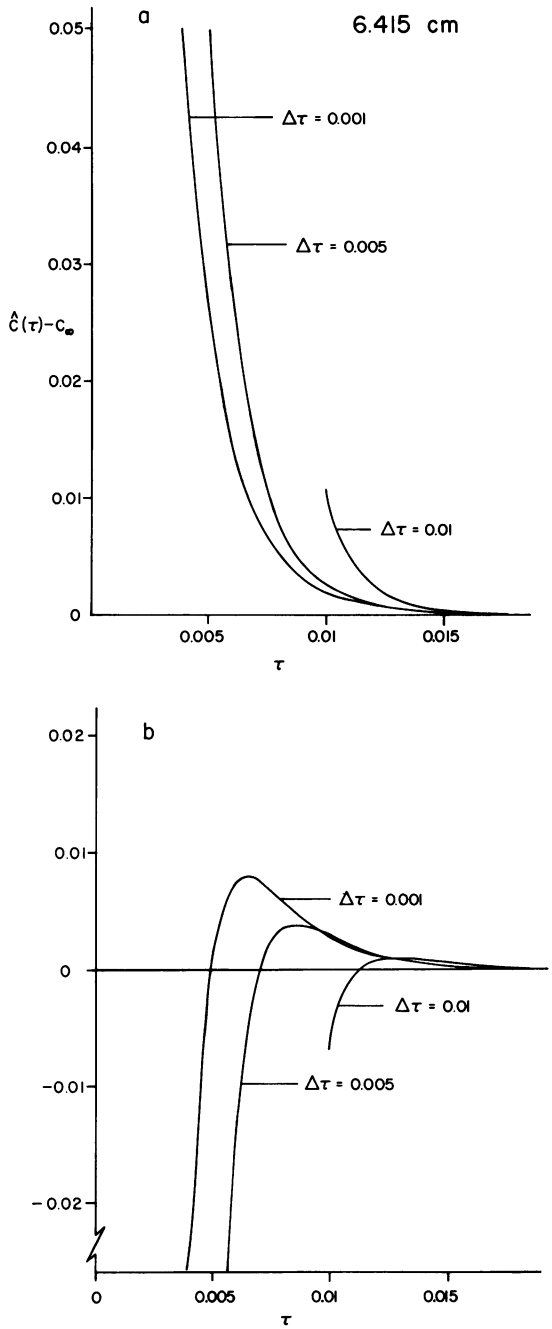

FIGURE 3 Differences between estimated and equilibrium concentrations as a function of the effective centrifugation time τ, illustrating the effects of changes in $\Delta\tau$, the spacing of the observation points. (*a*) At 6.415 cm, near the meniscus and (*b*) at 6.685 cm, near the base of the solution column.

TABLE I

COMPARISON OF TIMES REQUIRED TO ATTAIN EQUILIBRIUM WITH, τ'_ϵ AND WITHOUT, τ'_ϵ, APPLICATION OF THE DATA TRANSFORMATION. RESULTS ARE EXPRESSED IN UNITS OF τ

	kc_0		$\tau_{0.01}$	$\tau'_{0.01}$	$\tau_{0.001}$	$\tau'_{0.001}$
Simple nonideal systems with $s = s_0/(1 + kc)$; $\Delta\tau = 5 \times 10^{-3}$						
	0		0.040	0.008	0.061	0.009
$\alpha = 1$	0.25		0.040	0.008	0.061	0.010
	0.4		0.040	0.008	0.062	0.010
	1.0		0.041	0.008	0.062	0.011
$\alpha = 0.1$	0		0.144	0.079	0.205	0.110
	1.0		0.212	0.122	0.307	0.179
Ideal heterogeneous system; $\Delta\tau = 10^{-3}$						
α_1	α_2	ω_2^*				
1.0	0.5	0.1	0.045	0.006	0.069	0.014
		0.5	0.041	0.006	0.063	0.012
1.0	0.1	0.01	0.039	0.011	0.060	0.015
		0.1	0.035	0.015	0.055	0.019
		0.5	0.032	0.017	0.047	0.022
Self-associating systems; $\Delta\tau = 5 \times 10^{-3}$ except as indicated						
Monomer-dimer ($n = 2$)		kc_0^{N-1}				
		0.01	0.133	0.061	0.198	0.073
$\alpha_1 = 0.2$;		1.0	0.125	0.048	0.186	0.058
$\alpha_2 = 0.1$		1,000	0.100	0.054	0.172	0.076
		0.01‡	0.040	0.006	0.061	0.016
$\alpha_1 = 1$;		1.0‡	0.044	0.006	0.067	0.018
$\alpha_2 = 0.5$,		1,000	0.057	0.010	0.073	0.016
Monomer-hexamer, ($n = 6$)		0.01	0.168	0.078	0.243	0.098
$\alpha_1 = 0.2$		1.0	0.146	0.056	0.222	0.076
$\alpha_2 = 0.033$		1,000	0.100	0.055	0.162	0.077
		0.01	0.043	0.007	0.066	0.018
$\alpha_1 = 1$		1.0‡	0.052	0.015	0.079	0.020
$\alpha_2 = 0.167$		1,000	0.046	0.016	0.067	0.023

*ω_2 is the weight fraction of species 2 present in the original loading solution.
‡$\Delta\tau = 10^{-3}$.

This transformation appears to be useful even for heterogeneous systems, as illustrated in Fig. 4. Here we present the approach to equilibrium for both $c(\tau)$ and $\hat{c}(\tau)$, again using the van Holde-Baldwin criterion, for a system with 10% (Fig. 4 *a*) and 50% (Fig. 4 *b*) of a dimer ($\alpha = 0.5$) present in the initial sample. In all examples the sedimentation coefficient of any species was assumed to be proportional to the $\frac{2}{3}$ power of the molecular weight. The transformation appears to provide somewhat less reduction in equilibrium times than for an ideal single-component system but there is still more than a twofold savings in time. Similar behavior was noted for the presence of up to 50% of a decamer ($\alpha = 0.1$), as shown in Table I.

The Aitkens transformation provides significant time savings for ideal self-associating systems in rapid chemical equilibrium, as illustrated in Fig. 5 *a* for dimerization

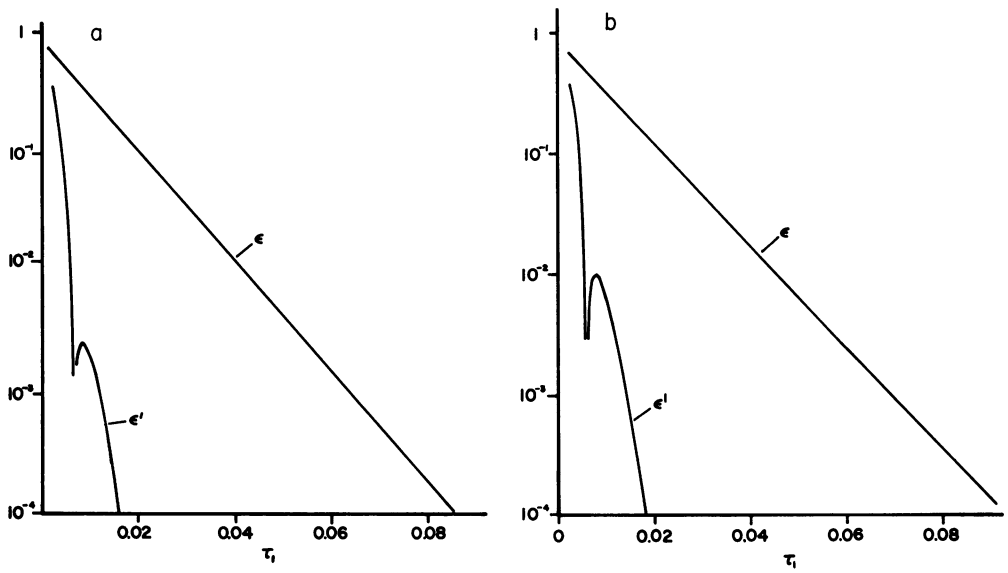

FIGURE 4 Comparison of the approach to equilibrium for observed c and estimated c concentrations, utilizing the van Holde-Baldwin criterion for ideal heterogeneous systems. The values of $\epsilon = |\Delta c_\tau - \Delta c_\infty| / \Delta c_\infty$ and of $\epsilon' \equiv |\Delta \hat{c}_\tau - \Delta c_\infty|$ are presented on a logarithmic scale as a function of τ. The data were calculated for compositions of the initial solutions (*a*) 90% monomer ($\alpha = 1$) and 10% dimer ($\alpha = 0.5$) and (*b*) equal amounts of monomer and dimer. Note that these systems are purely heterogeneous and that there is *no* chemical equilibrium between molecular species, nor any other expression of nonideality.

and in Fig. 5 *b* for a monomer-hexamer equilibrium for dimensionless association constants (kc_0^{n-1}) of unity. Table I includes, in addition, the relative equilibrium times for other values of the equilibrium constants for the self-association. It is seen that the savings in time are only modest functions of the specific conditions assumed and that substantial time savings are possible for all the types of cases considered.

CONSIDERATIONS OF RANDOM ERRORS

Fig. 6 shows the effect on the extrapolation procedure of random Gaussian noise added to the concentration. The random variables have mean equal to 0 and various standard deviations ranging from $10^{-3}\, c_0$ to $10^{-5}\, c_0$. Typical random errors in good experiments with the Rayleigh interference optics range from $3 \times 10^{-4} c_0$ to $3 \times 10^{-3} c_0$. Equilibrium experiments with the usual absorption optics exhibit random errors in the measured concentration distributions of $\sim 10^{-2} c_0$, at best, and the schlieren optics provide data with intermediate dispersion. It is apparent that the uncertainties in $\hat{c}(\tau)$ depend strongly on the values of $\Delta\tau$, the dimensionless time spacing of the data points used.

A straightforward analysis of the effects of random errors, δc_i, in the observed transient concentrations can be carried out. We assume that the concentrations at any radial point decay exponentially towards their equilibrium value (as in Eq. 3 with

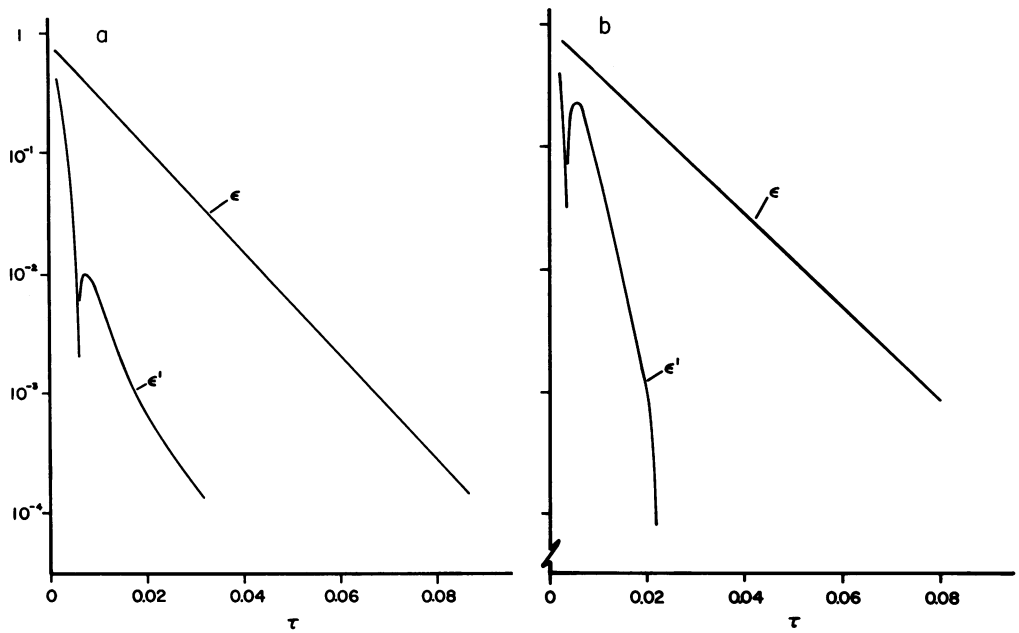

FIGURE 5 Comparison of the approach to equilibrium for reversibly associating ideal systems. Again ϵ and ϵ' are presented as a function of τ. In this case the systems are assumed to be ideal and homogeneous (in the thermodynamic sense) and exhibiting a rapid equilibrium (*a*) between monomer ($\alpha = 1$) and dimer ($\alpha = 0.5$) with a dimensionless association constant (kc_0) equal to unity and (*b*) between monomer ($\alpha = 1$) and hexamer ($\alpha = 0.167$) with $kc_0^5 = 1$.

$R_n \sim 0$) and that the δc_i are uncorrelated. The effects of these random errors on a predicted equilibrium concentration are given by

$$\delta \hat{c}_n = \frac{q_n(2\delta c_n - \beta\delta c_{n+1} - \delta c_{n-1}/\beta) + (\delta c_n)^2 - \delta c_{n-1}\delta c_{n+1}}{q_n(2 - \beta - 1/\beta) + 2\delta c_n - \delta c_{n-1} - \delta c_{n+1}}, \qquad (12)$$

where $q_n = A\beta^n$. The deviations, $\delta \hat{c}_n$, of the predicted equilibrium concentrations are obtained by the usual addition of squares as:

$$\delta \hat{c}_n^2 = (\partial \hat{c}_n/\partial c_{n+1})^2 \delta c_{n+1}^2 + (\partial \hat{c}_n/\partial c_{n-1})^2 \delta c_{n-1}^2 + (\partial \hat{c}_n/\partial c_n)^2 \delta c_n^2, \qquad (13)$$

or, on the average

$$<\delta c_n>^2 = \{(\partial \hat{c}_n/\partial c_{n+1})^2 + (\partial \hat{c}_n/\partial c_{n-1})^2 + (\partial \hat{c}_n/\partial c_n)^2\} <\delta c>^2 \qquad (14)$$

FIGURE 6 Illustrations of the effects of random errors on the Aitken estimation of the equilibrium concentrations. The curves indicate the actual values of concentration distribution as a function of τ, the effective centrifugation time. The indicated points were obtained from Eq. 2 with the concentration distributions calculated by solution of the Lamm equation (for $r = 6.415$ cm and $\alpha = 1$), perturbed by the addition of sets of random Gaussian deviates of various standard deviations so as to simulate various degrees of experimental error. In these panels: (*a*) $\Delta\tau = 10^{-2}$, SD = $10^{-3}c_0$; (*b*) $\Delta\tau = 5 \times 10^{-3}$, SD = $10^{-3}c_0$; (*c*) $\Delta\tau = 3 \times 10^{-3}$, SD = $10^{-5}c_0$; (*d*) $\Delta\tau = 10^{-3}$, SD = $10^{-4}c_0$.

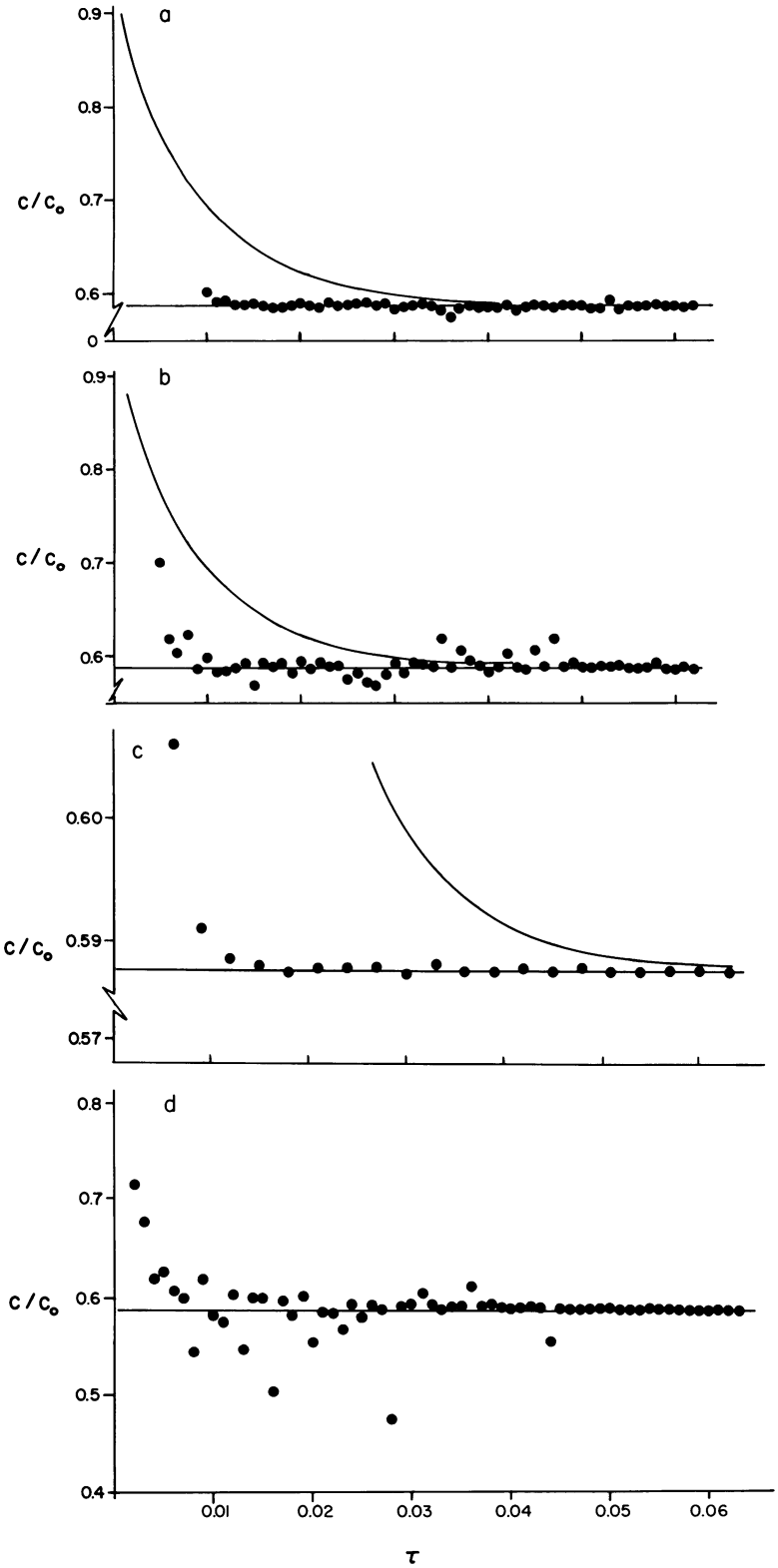
a
b
c
d
c / c₀
0.9
0.8
0.7
0.6
0
0.60
0.59
0.57
0.5
0.4
0.01
0.02
0.03
0.04
0.05
0.06
τ

where $<\delta c>$ represents the root mean square (rms) deviation of the experimental observations and $<\delta c_n>$ the rms deviation of the predicted equilibrium concentration. If we are sufficiently far from equilibrium so that $|q_n| = |A\beta^{n-1}| \gg |\delta c_i| / (1 - \beta)^2$, we then evaluate the ratio of errors

$$\frac{<\delta \hat{c}_n>}{<\delta c>} = 1/\eta(\beta) = (\beta^4 + 4\beta^2 + 1)^2/(1 - \beta)^2 \sim \sqrt{6}/(1 - \beta)^2, \quad (15)$$

where the approximation is valid for $\beta \sim 1$ and where

$$\beta = \exp(-\lambda \Delta\tau) = (c_{n+1} - c_\infty)/(c_n - c_\infty) = (c_n - c_\infty)/(c_{n-1} - c_\infty)$$

is the ratio of the transient portions of successive observed concentrations at uniform time intervals of $\Delta\tau$. Eq. 15 (presented in Fig. 7) represents the ratio of the rms error in the predicted equilibrium concentration to the rms error of the individual transient observation.

When $|q_n| \ll |\delta c_i|$, we are effectively at equilibrium and, although Eq. 2 may still be used to provide estimates of c_∞, it is simpler and more profitable to average successive values of the observed concentration, c_n. The intermediate case where

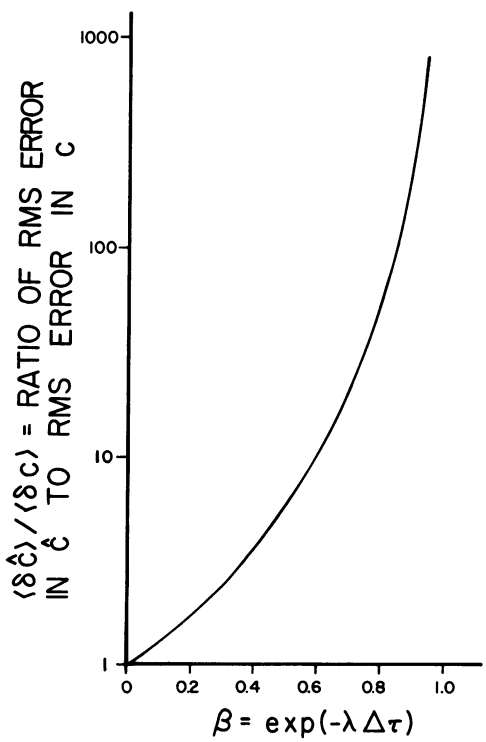

FIGURE 7 Effects of random error on the predicted concentrations. The ratio of the rms error in the predicted concentrations to the rms error in the observed concentrations is presented as a function of β, the ratio of successive remnant terms (see text for details).

$q_n \sim \delta c_i/(1 - \beta)^2$ is of interest, since the denominator of Eq. 12 can then tend to vanish for appropriate combinations of the δc_i and lead to large values for $|\delta c_n|$. This is illustrated in Fig. 8 *a*, where each indicated point represents the values of $<\delta\hat{c}>$ calculated from 100 sets of random Gaussian values for the δc_i in Eq. 12 with $\beta = \frac{2}{3}$ for each specific value of $q_n/<\delta c>$. The results from several such sets of simulated error calculations for different β ($0.5 < \beta < 0.9999$) can be summarized as essentially a single curve: Fig. 8 *b* presents these results in normalized form as $\eta(\beta) \cdot <\delta\hat{c}>/<\delta c>$ vs. $\eta(\beta)q_n/<\delta c>$ where the normalization factor $\eta = <\delta c>/<\delta\hat{c}>$ is defined in Eq. 15 as a function of β. The dashed lines in Fig. 8 correspond to $<\delta c> = q_n$. Obviously there is little point to using the $\hat{c}_n$ when $<\delta\hat{c}>$, the rms uncertainty of the estimated equilibrium concentration, is comparable to or greater than the remnant term q_n. Thus, the useful range for the application of the Aitken transformation (Eq. 2) is the area below the dashed line of Fig. 8 *b*.

From Fig. 8 *b* we also infer that the range of validity of Eq. 15 is $q_n > \sim 5/\eta$. For $q_n < \sim 5/\eta$ the values of $<\delta\hat{c}>$ increase rapidly by as much as two or three orders

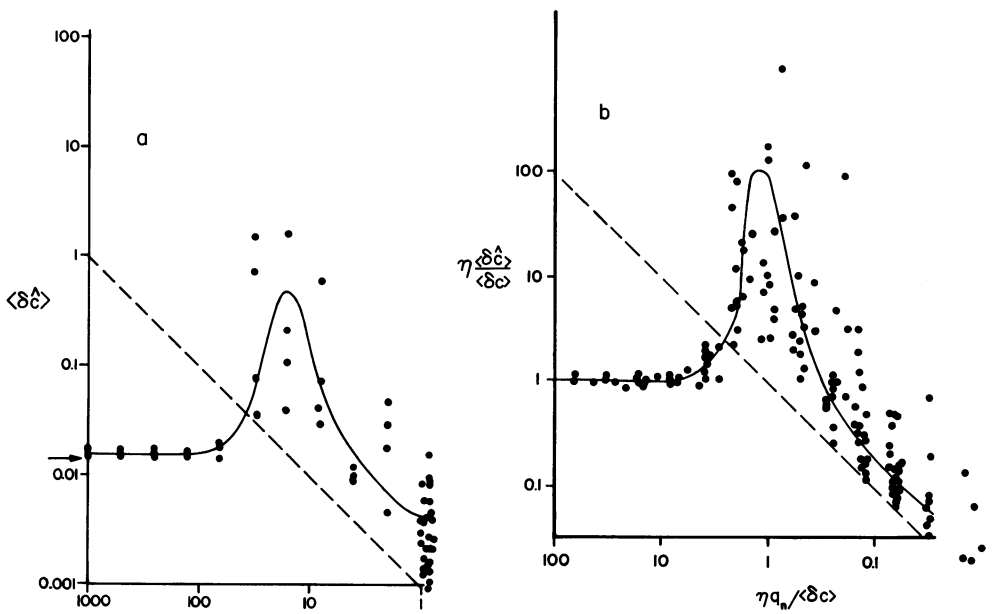

FIGURE 8 Monte Carlo simulations of the rms error in the predicted concentrations for various magnitudes of remnant terms, q_n. (*a*) The directly calculated values of $<\delta\hat{c}>$ obtained for β (ratio of successive remnant terms) = 0.67. Each point indicates the rms value of the $\delta\hat{c}_n$ given by Eq. 12 for 100 Gaussian values of the δc_i with $<\delta c> = 10^{-3}$ and plotted as a function of $q_n/<\delta c>$. (*b*) Normalized presentation of several sets of simulations of the $<\delta\hat{c}>$. Curves similar to those of panel *a* for several values of β ranging from 0.5 to 0.9999 are made coincident by multiplication of the ordinate by $\eta/<\delta c>$ and of the abscissa by η, where η is the inverse of the error ratio predicted by Eq. 7 for large remnant terms, q_n, in comparison with the δc_1. The limiting value of unity for $\eta<\delta\hat{c}>/<\delta c>$ at large q_n confirms the validity of Eq. 7 for $\eta q_n \sim 5 <\delta c>$. Note the spectacular increase in the error ratio as the remnant term vanishes. (The indicated curve is intended only as a summary of the data).

of magnitude. In the limit, as $|\delta c_i| \gg |q_n|$, the values of the $|\delta \hat{c}_n|$ become, on the whole, smaller, with the exception of sporadic outlying points. The distribution function for these $\delta \hat{c}_n$ has been estimated by a Monte Carlo procedure. The distribution appears to have a tail extending to rather large values and the tail of this distribution is so significant that there appears to be no limiting value for the apparent values of $<\delta \hat{c}>$ as more and more points are taken to evaluate the $<\delta \hat{c}>_{app}$. It is interesting to note, however, that truncation of the tail of this distribution at arbitrary limits does give satisfactory limits to the $<\delta \hat{c}>_{app}$, with the magnitudes of these $<\delta \hat{c}>_{app}$ being proportional to the square root of the arbitrary truncation limits that were used! If $f(x)$ is the probability density of the error, then this empirical result implies that $f(x)$ is proportional to $1/x^2$ for large x.

As shown by Fig. 3 and Eq. 10, the rate of approach of the $c(\tau)$ to the equilibrium concentration, c_∞, depends strongly on $\Delta\tau$, the time interval between the concentration determinations. We have also seen that the magnitude of $<\delta \hat{c}>$ does strongly depend on the values of $\Delta\tau$. Fig. 9 presents equilibration times τ'_ϵ calculated from Eq. 10 for $\alpha = 1$ and $\epsilon = 10^{-3}$ as a function of $\Delta\tau$. The corresponding values of

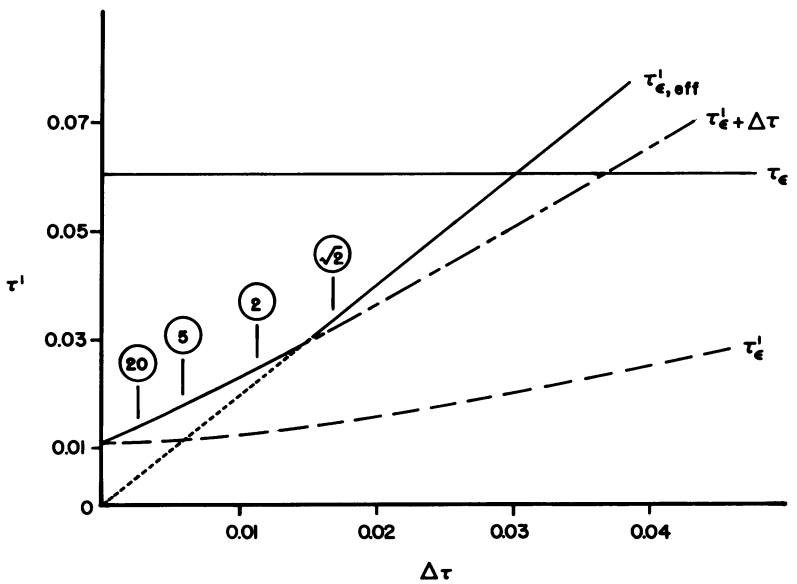

FIGURE 9 Total effective equilibration time, τ', as a function of $\Delta\tau$ for $\alpha = 1$ and $\epsilon = 10^{-3}$. The usual equilibrium time given by the van Holde-Baldwin relation, Eq. 8, is indicated by the horizontal line marked τ_ϵ. The corresponding time required to estimate Δc_∞ within $\epsilon = 10^{-3}$ as given by Eq. 10 is the dashed line indicated τ'_ϵ. When τ'_ϵ is greater than $\Delta\tau$, the total time required for $\Delta \hat{c}_\tau$ to approximate Δc_∞ within ϵ is given by the solid segment of the line marked $\tau'_\epsilon + \Delta\tau$. When τ'_ϵ is less than $\Delta\tau$, the total time required is $2\Delta\tau$ and is indicated by the solid segment of the straight line ($\tau' = 2\Delta\tau$) through the origin. Thus the total effective equilibration time is represented by the two solid line segments marked $\tau'_{\epsilon,\text{eff}}$. The encircled numbers indicate the values of $<\delta \hat{c}>/<\delta c>$, the ratio of the rms error in $\Delta \hat{c}$ to the rms observation error in c for the several values of $\Delta\tau$.

$<\delta\hat{c}>/<\delta c>$ are indicated adjacent to several points. The corresponding time to attain equilibrium by the van Holde-Baldwin equation (Eq. 8) is also indicated as τ_ϵ.

Each application of Eq. 2 requires three determinations of $c(r, \tau)$: at τ_n, and at $\tau_n \pm \Delta\tau$. The time required is thus $\tau_n + \Delta\tau$ or, $2\Delta\tau$ when $\tau_n < \Delta\tau$, since only positive values of τ exist. To ensure convergence within ϵ, $\tau \geq \tau'_\epsilon$. Accordingly the minimum time required to obtain a value $\Delta\hat{c}(\tau)$ within ϵ of $\Delta c_\infty(r)$ is $\tau'_\epsilon + \Delta\tau$ when $\tau'_\epsilon > \Delta\tau$ and $2\Delta\tau$ when $\tau'_\epsilon < \Delta\tau$, as illustrated by the solid curve marked $\tau'_{\epsilon,\text{eff}}$ in Fig. 9. This minimum time may be considered to be a function of the ratio of errors $<\delta\hat{c}>/<\delta c>$. The maximum practically attainable reduction in the time required to estimate the equilibrium concentration distribution within any given error may thus be estimated.

The maximum practically attainable reduction in equilibration time, $\tau'_{\epsilon,\text{eff}}/\tau_\epsilon$, is presented as a function of $1/\alpha$ for various indicated error ratios in Fig. 10 for $\epsilon = 10^{-3}$. For error ratios more than about 10, the reduction in equilibration time is only a weak function of the error ratio. For smaller error ratios one must use a greater value of $\Delta\tau$ and thus increase the effective equilibration time needed. In general it should be noted that, after an initial region where the maximum saving is greatest and independent of α, the time saving decreases with increasing molecular weight or centrifuge speed. However, it should also be noted that the usual equilibration times are considerably smaller for higher speeds (see ref. 14).

The curves corresponding to those presented in Fig. 10 but for $\epsilon = 10^{-2}$ and

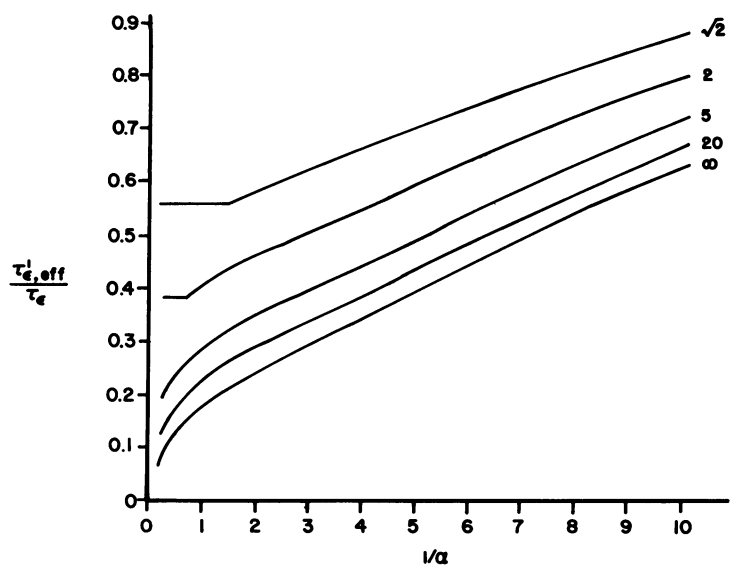

FIGURE 10 Ratios of the total effective equilibration time needed to estimate equilibrium within $\epsilon = 10^{-3}$ to the van Holde-Baldwin time τ_ϵ. The several curves represent the practical reduction in the time required to estimate equilibrium for the indicated rms error ratio. Note that the usual low-speed equilibrium experiments are generally carried out for $\alpha \leq \sim 1$.

$\epsilon = 10^{-4}$ are similar. The curves for small $\delta\tau$ have been presented as Fig. 1 and there are only minor changes with ϵ for $\alpha < 1$ in the limiting behavior for large error ratios. The branches in the curves for specified error ratios occur at higher values of $\tau'_\epsilon/\tau_\epsilon$ for $\epsilon = 10^{-2}$ and at lower values of $\tau'_\epsilon/\tau_\epsilon$ for $\epsilon = 10^{-4}$ than shown in Fig. 10. This is to be expected since a smaller value of ϵ always implies a larger centrifugation time and thus permits greater values of $\eta\Delta\tau$ and results in smaller values of $<\delta\hat{c}>/<\delta c>$.

We have therefore seen that there is considerable potential in the use of the Aitken transformation for reducing equilibrium times in sedimentation experiments. An advantage in using this method for reducing running times is that no system parameters need be known, in contrast to other overspeeding techniques. Furthermore, the extrapolation procedure works well for nonideal systems. A principal drawback is the technique's susceptibility to noise. We are presently investigating the use of different data-smoothing procedures to overcome the difficulties presented by noisy data.

This work has been supported, in part, by grants BMS 71-01299 and PCM 76-21847 from the National Science Foundation. Numerical computations were performed at the University of Connecticut Computer Center, which has been supported, in part, by grant GJ-9 from the National Science Foundation.

Received for publication 1 April 1977 and in revised form 20 July 1977.

REFERENCES

1. VAN HOLDE, K. E., and R. L. BALDWIN. 1958. Rapid attainment of sedimentation equilibrium. *J. Phys. Chem.* **62**:734–743.
2. YPHANTIS, D. A. 1960. Rapid determination of molecular weight of peptides and proteins. *Ann. N. Y. Acad. Sci.* **88**:586–601.
3. HEXNER, P. E., L. E. RADFORD, and J. W. BEAMS. 1961. Achievement of sedimentation equilibrium. *Proc. Natl. Acad. Sci. U. S. A.* **47**:1848–1852.
4. TELLER, D. C., R. A. HORBETT, E. G. RICHARDS, and H. K. SCHACHMAN. 1969. Ultracentrifuge studies with Rayleigh interference optics. III. Computational methods applied to high speed sedimentation equilibrium experiments. *Ann. N. Y. Acad. Sci.* **164**:66–101.
5. GRIFFITH, O. M. 1967. Rapid sedimentation equilibrium in the ultracentrifuge using a modified synthetic boundary cell with step concentrations. *Anal. Biochem.* **19**:243–248.
6. BAURAIN, R. M., J. C. MOREUX, and F. LAMY. 1973. Rapid preequilibrium determination of molecular weights in the ultracentrifuge. *Biochim. Biophys. Acta.* **295**:18–29.
7. ARCHIBALD, W. J. 1942. The integration of the differential equation of the ultracentrifuge. *Ann. N. Y. Acad. Sci.* **43**:211–227.
8. WEISS, G. H., and D. A. YPHANTIS. 1965. Rectangular approximation for concentration-dependent sedimentation in the ultracentrifuge. *J. Chem. Phys.* **42**:2117–2123.
9. DISHON, M., G. H. WEISS, and D. A. YPHANTIS. 1966. Numerical solutions of the Lamm equation. II. Equilibrium sedimentation. *Biopolymers.* **4**:457–468.
10. AITKEN, A. C. 1926. On Bernoulli's numerical solution of algebraic equations. *Proc. R. Soc. Edinb.* **46**: 289–305.
11. RALSTON, A. 1965. A First Course in Numerical Analysis. McGraw-Hill Book Company, New York.
12. SHANKS, D. 1955. Non-linear transformations of divergent and slowly convergent sequences. *J. Math. Phys.* **34**:1–42.
13. DISHON, M., G. H. WEISS, and D. A. YPHANTIS. 1966. Numerical solutions of the Lamm equation. I. Numerical procedure. *Biopolymers.* **4**:449–455.
14. YPHANTIS, D. A. 1964. Equilibrium ultracentrifugation of dilute solutions. *Biochemistry.* **3**:297–317.